eISSN: 2721-5717; pISSN: 2747-2124 https://journal.unhas.ac.id/index.php/zonalaut

ZONA LAUT

JURNAL INOVASI SAINS DAN TEKNOLOGI KELAUTAN

Dynamic Response Analysis of a Decommissioning Barge

Anggoronadhi Dianiswara[1*], Destyariani Liana Putri[1], Alamsyah[2], Muhammad Khaisar Wirawan[1], Nurmawati[1], Hasrina[1]
[1]Departement of Ocean Engineering. Kalimantan Institute of Technology, Indonesia
[2]Departement of Naval Architecture. Kalimantan Institute of Technology, Indonesia
*anggoronadhi@lecturer.itk.ac.id

Abstract

The decommissioning of offshore platforms is an important stage in the life cycle of offshore structures to prevent environmental impacts and navigation hazards. In Indonesia, many aging platforms require removal. However, the high operational costs remain a major challenge. This study aims to analyze the dynamic response of a 400 ft flat top barge converted into a decommissioning barge by adding an upending frame and modifying the stern geometry into a fork-like shape, allowing it to replace the conventional crane barge. A time-domain analysis was conducted to evaluate the dynamic motion of the barge and mooring line tension under irregular wave conditions with wave approach angles of 0°, 45°, 90°, 135°, and 180°. The results indicate that the barge experiences dominant responses at low frequencies around 0.15 Hz, signifying a natural resonance that influences the heave, roll, and pitch motions. Comparison of mooring system performance between the stand-off and stand-on positions shows that the stand-on configuration provides more stable motion and evenly distributed line tension, while the stand-off condition results in larger lateral motions and higher tension fluctuations. Overall, the barge's dynamic motion and mooring system responses remain within safe operational limits, confirming that the modified barge is suitable for Abandonment and Site Restoration (ASR) activities.

Keywords: decommissioning barge, dynamic analysis, mooring system, time-domain, offshore platform

1. INTRODUCTION

Offshore platforms consist of several types, namely fixed offshore platforms and floating offshore platforms. There are 630 offshore platforms spread almost throughout Indonesia [1]. A total of 522 platforms are operational, 102 platforms are not operational, and 6 units are abandoned [2]. Referring to the Government Regulation of the Minister of Energy and Mineral Resources Number 15 of 2018 Article 2, Cooperation Contract Contractors (KKKS) are required to carry out post-operational activities to avoid negative impacts, such as disruption of shipping routes to damage to the ecosystem around the platform [3]. So it is necessary to decommission the offshore platform after operation. However, in the decommissioning process there are several challenges. Starting from the lack of reserve costs for old platforms, the need for effective and efficient technology, to simple and integrated regulations. The dismantling process generally involves 4 types of vessels, namely crane barges, flat top barges, anchor handling tugs, and tugboats. To save on crane barge rental costs, which amount to 3 billion rupiah per day, while also supporting an effective and efficient dismantling process, a 400-foot flat-top barge was converted into a decommissioning barge, replacing both the crane and the flat-top barge.

During decommissioning activities, wind, wave, and current conditions require the decommissioning barge to be moored to ensure it remains in its intended location and allows for safe decommissioning. However, as of 2014, 19% of the 107 mooring lines on 73 permanently moored floating structures had failed during the design phase [4]. One step in analyzing the dynamic response of the decommissioning barge and mooring lines is to comply with applicable standards [5], [6].

copyright is published under Lisensi Creative Commons Atribusi 4.0 Internasional.

Several literatures have examined the motion and mooring line response of crane barge. Investigation of dynamic non-linear motion using various mathematical approaches on floating cranes has been conducted [7], [14]. A study of the dynamic non-linear response of large-sized crane vessels to regular waves has been analyzed [8]. The dynamic response with flexible boom types and swing loads on cranes has been investigated previously [9]. Analysis of the mooring line response calculated quasistatically has been conducted [10]. To ensure the decommissioning barge's mooring system complies with applicable standards and avoids failure, an analysis similarity examinated in the previous study of crane barge [11] was conducted to obtain the dynamic response of the mooring line tension. From this analysis, it is known whether the tension of the designed mooring line meets the standards.

2. METHODS

2.1. Mooring Line Modelling

The motion of the mooring line elements is written in the following equation:

$$\frac{\overrightarrow{\partial \mathrm{T}}}{\overrightarrow{\partial \mathrm{S}_e}} + \frac{\overrightarrow{\partial \mathrm{V}}}{\overrightarrow{\partial \mathrm{S}_e}} + \vec{w} + \vec{F}_h = m\frac{\partial^2 \vec{R}}{\partial t^2} \quad (1)$$

$$\frac{\overrightarrow{\partial \mathrm{M}}}{\overrightarrow{\partial \mathrm{S}_e}} + \frac{\overrightarrow{\partial \mathrm{R}}}{\overrightarrow{\partial \mathrm{S}_e}} + \vec{V} = -q \quad (2)$$

Where:

m	= mass of structure per unit length
$\vec{q}$	= distribution of moment load per unit length
$\vec{R}$	= first node vector position of the mooring line element
∂S_e	= element length

The bending moment and tensile force are related to the bending stiffness EI and the axial stiffness EA of the mooring line material. This relationship is written by the equation.

$$M = EI\frac{\partial \vec{R}}{\partial \mathrm{S}_e} \times \frac{\partial^2 \vec{R}}{\partial S_e^2} \quad (3)$$

$$T = EA_\varepsilon \quad (4)$$

Where:

E	= axial strain of the additional rope element

2.2. Wave Force Modelling

The wave force is calculated by the boundary element method based on the diffraction theory, using Ansys Aqwa [12][15]. By ignoring the interaction between waves and currents, it is assumed that the first-order wave force of the floating structure consists of the wave excitation force and the radiation force, which can be linearly superposed. The wave excitation force consists of the incident force and the diffraction force. The radiation force can be considered as the added mass force and the radiation damping force. The potential equation of the first-order wave force is as follows:

$$\phi(X,Y,Z,t) = \phi(X,Y,Z)_e^{-iwt} \quad (5)$$

$$\phi(X,Y,Z)_e^{-iwt} = \left[(\phi_1 + \phi_D) + \sum_{j=1}^{6} \phi_j x_j\right] e^{-1wt} \quad (6)$$

Where:

ϕ_1	= potential that occurs
ϕ_D	= diffraction potential

copyright is published under Lisensi Creative Commons Atribusi 4.0 Internasional.

x_j = amplitude of freedom of motion j of the floating structure

The first-order potential velocity is substituted into the linear Bernoulli equation, so that the equation becomes:

$$p(X,t) = -p\frac{\partial \phi}{\partial t} \tag{7}$$

Adding the wave excitation force and radiation force, so that the first-order wave force (unit amplitude) on the floating structure is written as follows:

$$F = F_j + F_{ji} \tag{8}$$

$$F_j = -\int_s pIDn_j dS = -\int_s iwp\,(\phi_1 + \phi_D)n_j dS \tag{9}$$

$$F_{ji} = -\int_s p_i n_j dS = -\int_s iwp\,\phi_I n_j dS = -A_{ji}\ddot{x}_\iota - B_{ij}\dot{x}_\iota \tag{10}$$

Where:

F_j = wave excitation force in the j direction

F_{ji} = radiant force in the j direction caused by the free movement i of the floating structure

S = wetted surface of a floating structure

n_j = normal vector in the j direction

A_{ji}, B_{ij} = added mass and radiation attenuation coefficient

A_{ji} and B_{ji} if described, can be written as follows:

$$A_{ji} = \frac{\rho}{\omega}\int_s \phi_I m_j n_i dS \tag{11}$$

$$B_{ji} = \rho\int_s \phi_I Re(n_j) dS \tag{12}$$

Floating structures subjected to waves not only experience first-order wave forces consistent with the wave frequency, but also nonlinear second-order wave forces. The second-order wave force components consist of the average wave drift force, the low-frequency wave drift force, and the high-frequency wave drift force. The average wave drift force and the low-frequency wave drift force are proportional to the square of the incident wave amplitude, which is referred to as the Quadratic Transfer Function (QTF) of the second-order wave force.

$$F_{drift}^{x}(t) = \sum_{j=1}^{n}\sum_{k=1}^{n} Re\left\{Q_d^{(j,k)}(\omega_j,\omega_k)a_j a_k e^{i(\omega_j-\omega_k)t}e^{-i(\phi_j-\phi_k)}\right\} \tag{13}$$

Where:

$F_{drift}^{i}(t)$ = At i: 1, 2, 3, then the wave drift force in the x,y,z directions in the local coordinate system of the floating structure

$F_{drift}^{i}(t)$ = At i: 4, 5, 6, the wave drift moments of the x,y,z axes in the local coordinate system of the floating structurestructure

n = the number of waves divided into irregular waves

Q_d^i = represents the nth-order low-frequency QTF matrix in the i-direction of degrees of freedom

$Q_d^i(\omega_j,\omega_k)$ = low frequency wave force transfer function value of two regular waves with frequencies ω_j and ω_k in the QTF matrix

$a_j\ and\ a_k$ = amplitude of the j[th] and k[th] reguar waves

$\phi_j\ and\ \phi_k$ = the j[th] and k[th] regular wave phases

copyright is published under Lisensi Creative Commons Atribusi 4.0 Internasional.

If j = k, then it represents the average wave drift force. When j ≠ k, it represents the low-frequency wave drift force. By adding equations (8) and (13), the wave force on the floating structure can be written as follows:

$$F_{wave}^{i}(t) = F + F_{drift}^{i}(t) \tag{14}$$

2.3. Wind Force Modelling

The wind force on a floating structure can be calculated using the following equation:

$$F_{wind}^{i}(t) = C_{Wi}U_W(t)|U_W(t)|i = 1, \dots ,6 \tag{15}$$

Where:

$F_{wind}^{i}(t)$ = wind force in the x,y,z directions and wind torque around the x,y,z axes in the local coordinate system of the floating structure

C_{Wi} = wind force/moment coefficient corresponding to the angle of incidence of the wind load at time, t

$U_W(t)$ = real-time relative speed of wind and floating structures along the direction of wind propagation

2.4. Current Force Modelling

There are two types of current forces on floating structures, one that does not consider the interaction between waves and currents, and the other that considers wind, wave, and current loads. The current force equation, ignoring wave interaction [13], is as follows:

$$F_{current}^{i}(t) = C_{Ci}U_C(t)|U_C(t)|i = 1, \dots ,6 \tag{16}$$

Where:

$F_{wind}^{i}(t)$ = wind force in the x,y,z directions and wind torque around the x,y,z axes in the local coordinate system of the floating structure

C_{Wi} = wind force/moment coefficient corresponding to the angle of incidence of the wind load at time, t

$U_W(t)$ = real-time relative speed of wind and floating structures along the direction of wind propagation

The current force equation with a combination of wind, wave and current loads on the floating structure and its interaction with the mooring system, the platform motion equation, xj (t), in the time domain is written as follows

$$\sum_{j=1}^{6}[M_{ij} + m_{ij}]\ddot{x}_j(t) + \int_0^t R_{ij}(t-\tau)\dot{x}_j(\tau)d\tau + C_{ij}X_j(t) + K_{ij}x_j(t) = F_{wave}^{i}(t) + F_{wind}^{i}(t) + F_{current}^{i}(t) + F_{moor}^{i}(t) \tag{17}$$

Where:

M_{ij} = mass matrix of floating structures

m_{ij} = added mass matrix

R_{ij} = hysteresis function matrix

C_{Ci} = viscous damping matrix

K_{ij} = static recovery stiffness matrix of floating structures

$F_{wave}^{i}(t)$ = wave force vector

$F_{wind}^{i}(t)$ = wind force vector

$F_{current}^{i}(t)$ = current force vector

$F_{moor}^{i}(t)$ = mooring system force vector

copyright is published under Lisensi Creative Commons Atribusi 4.0 Internasional.

Based on the convolution method, the added mass matrix (mij) and delay function matrix (Rij) can be obtained with the added mass coefficient (Aij) and radiation attenuation coefficient (Bij) obtained from hydrodynamics.

$$m_{ij} = A_{ij}(\infty) \tag{18}$$

$$B_{ij} = \frac{2}{\pi}\int_0^\infty B_{ij}\,(\omega)\cos(\omega t)\,d\omega \tag{19}$$

2.5. Decommissioning Barge and Mooring Line

To convert the 400 ft flat top barge into a decommissioning barge, an upending frame was added to lift and handle platform structures to be dismantled. The stern was modified into a fork-like geometry to facilitate the decommissioning process. Additional equipment was also installed to support maximum operation efficiency. The dimensions of the decommissioning barge can be seen in table 1 below.

Table 1. Decommissioning Barge Dimensions

No	Parameter	Value	Unit
1	Length (LoA)	122	meter
2	Breadth (B)	36.6	meter
3	Height	7.625	meter
4	Draft (D)	4.5	meter

A dynamic analysis was performed to determine the barge's motion response and its mooring system behavior under irregular wave conditions using a time-domain approach. The environmental data used in the simulation are shown in Table 3. The mooring line used was a 28.00 mm (6x36 IWRC Steel Wire Rope) with a weight of 575 kg/m, a Maximum Breaking Load (MBL) of 92.8 MT, and an actual length of 1200 m. The mooring arrangements for stand-off and stand-on positions are presented in Table 2.

Table 2. Mooring arrangement

Mooring Line	Azimuth Deg (°)	Anchor Radius
Stand off		
P1	36.5	675
P2	70.05	737
P3	128.53	885
P4	154.52	933
S1	323.5	675
S2	289.95	737
S3	231.47	885
S4	205.48	933
Stand on		
P1	30	800
P2	60	800
P3	120	800
P4	150	800
S1	330	800
S2	300	800
S3	240	800
S4	210	800

copyright is published under Lisensi Creative Commons Atribusi 4.0 Internasional.

Table 3. Environmental Data

Irreguler wave	
Significant Wave Height	1.85 m
Peak Period	6.177 s
Gamma	1.694
Wind	
1 min wind speed	14.84 m/s
Current	
Vector sum current speed	0.62 m/s

3. RESULTS AND DISCUSSION

3.1. Respon Amplitudo Operator (RAO)

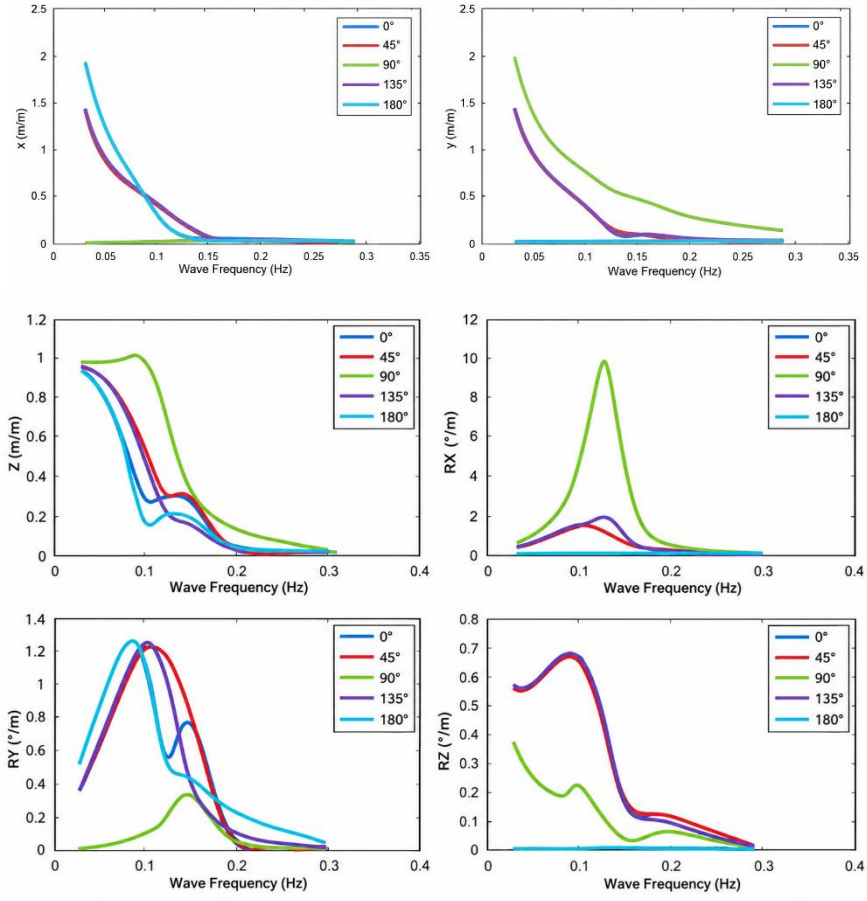


Figure 1. RAO Decommissioning Barge Graph

The Response Amplitude Operator (RAO) plots describe the barge's response to wave frequencies at different angles of incidence. The longitudinal (X) and transverse (Y) translation plots show the greatest response at low frequencies, below 0.1 Hz, with amplitude decreasing with increasing frequency. This indicates that the barge is more susceptible to movement at long (low-frequency) waves. However, a secondary peak is observed around 0.15 Hz, indicating possible resonance. This peak corresponds to the barge's natural period, where the structure experiences maximum response despite the relatively small wave amplitude.

The vertical translation (Z) or heave plots show a similar pattern, with the highest response at low frequencies and a second peak around 0.15 Hz. These peaks are more pronounced at 0° and 45° angles, indicating that frontal and diagonal waves have the greatest impact on the barge's vertical motion. The resonance at these frequencies suggests that the barge could experience significant heaving when the wave period approaches the barge's natural period, potentially increasing the risk of instability.

copyright is published under Lisensi Creative Commons Atribusi 4.0 Internasional.

On the rotation graph, the roll response (RX) shows a sharp peak around 0.1 Hz, with a second, smaller peak around 0.15 Hz, particularly at 45° and 90° angles. This indicates that the barge is highly sensitive to side waves, with resonance contributing to increased roll amplitude. Pitch rotation (RY) shows a main peak around 0.2 Hz, slightly higher than the translational resonance peak, indicating that frontal waves have a significant influence on pitch motion, particularly as they approach the secondary resonance frequency.

Yaw (RZ) exhibits a consistent pattern with a low-frequency peak and a small resonance around 0.15 Hz, indicating the influence of side and diagonal waves on the barge's horizontal rotation. This analysis indicates that the barge's natural period, around 0.15 Hz, plays a significant role in determining safe and stable operating conditions. The presence of this resonance peak suggests that operational design and decommissioning scheduling should take environmental wave frequencies into account to avoid resonance conditions that could increase the risk of extreme motion and instability

The results showed that the pressure drop in the hydraulic windlass system on MV. The performance of the anchor retrieval was impacted by Talent Blu. In the anchor heave-up operation at Sidor Port, Venezuela on 30 September 2024, the problem arose. The hydraulic windlass had a working pressure of 15.7 MPa, anchor lifting speed of 9 m/min, rated load of 181 kN and drum speed of 8.5 rpm under normal conditions. When the incident occurred, the anchor speed reduced to about 4-5 m/min and the drum speed could not be above 4 rpm even with the remote control set to the maximum. There were also abnormal noises and vibration observed around the windlass unit.

3.2. Barge Motions

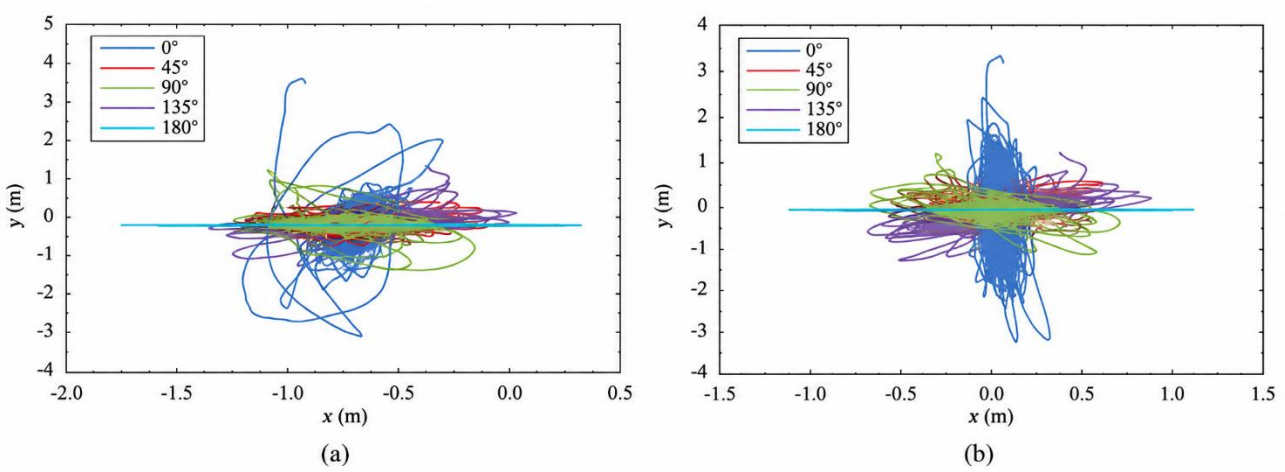


Figure 2. Decommissioning Barge Motions: (a) Stand off (b) Stand on

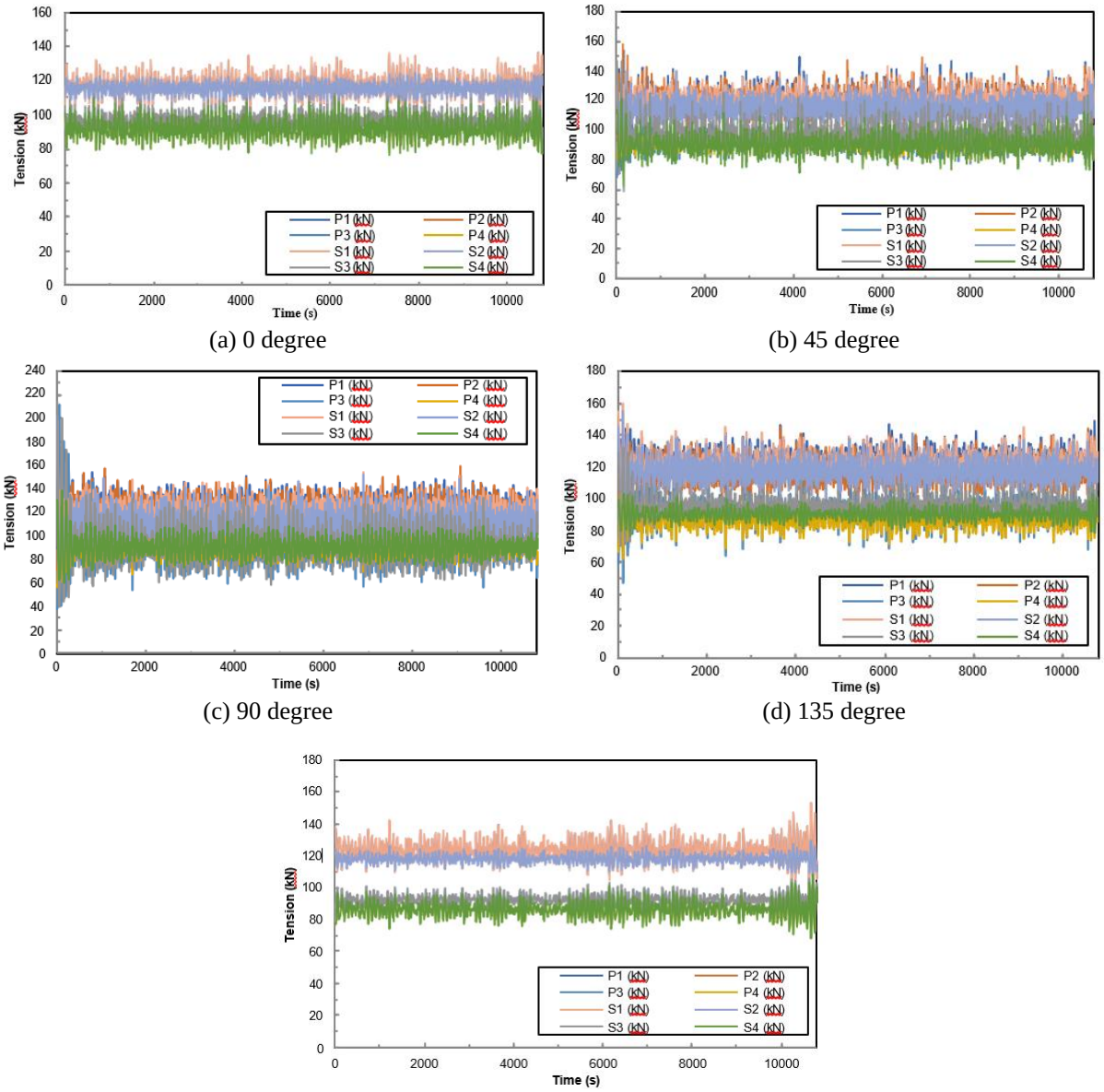
Based on Figure 1, the barge motion graph shows the difference in movement between the stand-off (a) and stand-on (b) positions, which is influenced by the mooring line. Figure (a) shows that the barge's movement is larger and more dispersed, especially at wave angles of 90° and 135°. This occurs because the mooring line is relatively slack, which reduces tension and allows the barge to move more freely under the influence of the waves. This movement indicates that the barge is more susceptible to significant lateral shifts when it is far from the platform or main structure.

However, in contrast, in Figure (b), the barge's movement appears more concentrated and stable. This is due to the increased tension in the mooring line as the barge approaches the platform. This tension serves to prevent large lateral movements and keeps the barge close to the platform during decommissioning operations. Wave angles of 0° and 45° show smaller amplitudes of movement, indicating that the mooring system effectively controls the barge's movement. Based on this pattern, it is known that the importance of adjusting the tension mooring line in maintaining the stability of the barge and preventing the risk of collision or unwanted shifting during operations around the platform.

copyright is published under Lisensi Creative Commons Atribusi 4.0 Internasional.

3.3. Dynamic Mooring Line Tension

3.3.1. Stand Off (Position A)



(a) 0 degree

(b) 45 degree

(c) 90 degree

(d) 135 degree

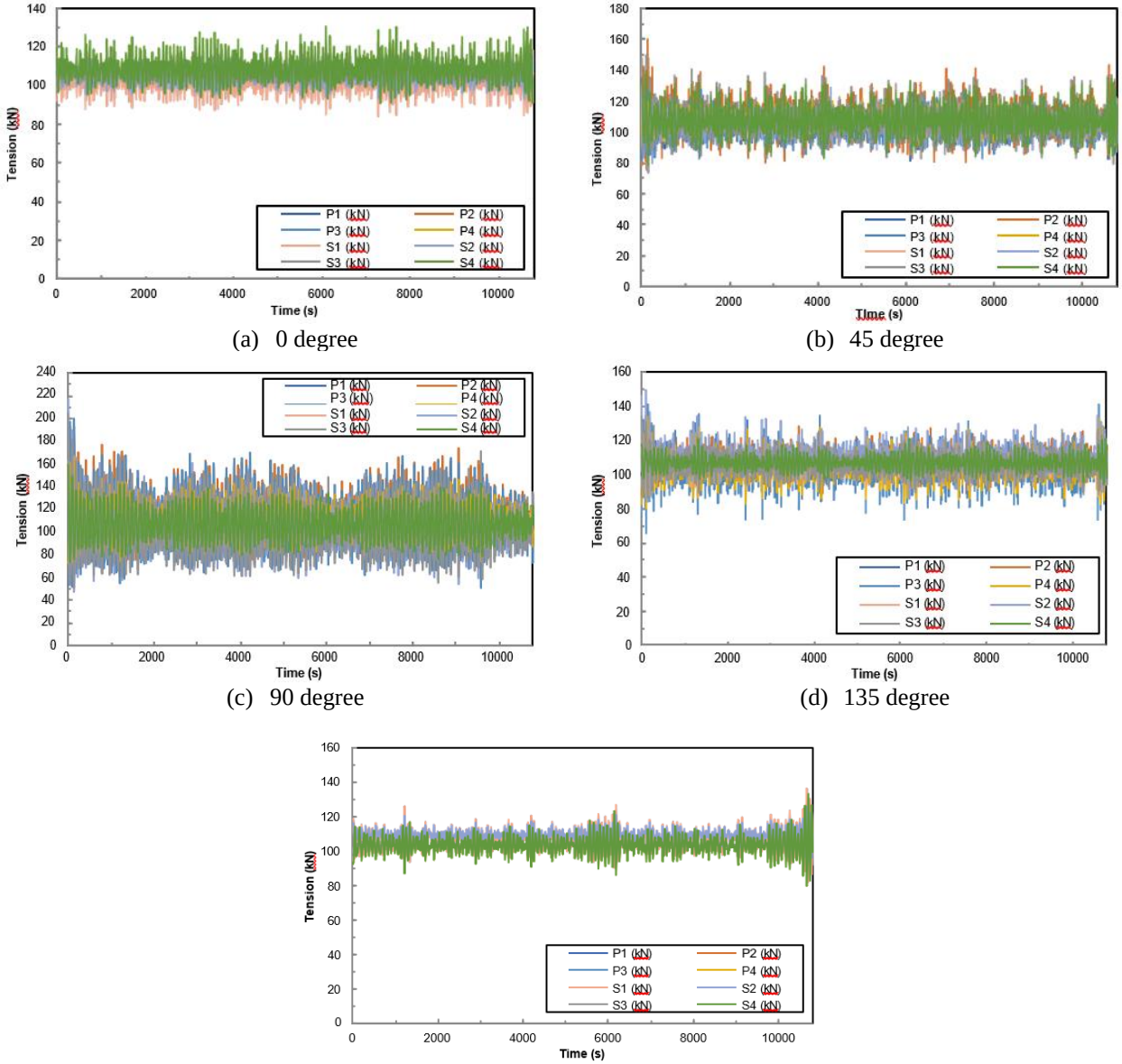
(e) 180 degree

Figure 3. Mooring Line Tension Position Stand Off

The graphs above illustrate how the mooring line responds to various wave angles: 0°, 45°, 90°, 135°, and 180°, over a period of time. In the stand off position, tension fluctuations at 90° and 135° appear larger and more irregular. The tension force range shows higher values, reaching 200 kN in some graphs. Tensions between the mooring line on the port (P1-P4) and starboard (S1-S4) sides also appear to vary, indicating uneven force distribution. This indicates that the mooring line is in a slack condition, allowing the barge to move more freely under the influence of the waves. Larger lateral and longitudinal movements cause the tensile force on the mooring line to change significantly, especially when waves come from the side or diagonally.

copyright is published under Lisensi Creative Commons Atribusi 4.0 Internasional.

3.3.2. Stand On (Position B)



(a) 0 degree (b) 45 degree

(c) 90 degree (d) 135 degree

(e) 190 degree

Figure 4. Mooring Line Tension Position Stand On

The Stand on position provides more stable tension fluctuations compared to the Stand off position. Mooring line tension in this position tends to be below 150 kN. Tension on both sides of the barge, both Port and Starboard, shows a more even force distribution, indicating that the mooring line is in a tighter condition. Thus, the barge has a more controlled movement, reducing the risk of large lateral movements when near the platform. This stability is very important during decommissioning operations that require high precision. From the perspective of wave direction, the graph shows that at 0° and 180° angles, tension fluctuations are relatively small because the waves come from the front or rear, so the barge moves parallel to the wave direction. Angles of 45° and 135° show moderate fluctuations reflecting a combination of heave, pitch, and roll movements. However, at an angle of 90°, the highest tension occurs, especially in the Stand-Off position, because waves from the side have a significant impact on the barge's roll and sway movements.

Therefore, it can be concluded that the Stand On position (Position B) produces a more stable and even tension distribution than the Stand Off position (Position A). This indicates that maintaining the mooring line in a taut condition is crucial to ensure barge stability during operation. In the Stand Off position, greater tension fluctuations indicate that the mooring line must be designed to withstand high loads, especially at angles of 90° and 135°.

copyright is published under Lisensi Creative Commons Atribusi 4.0 Internasional.

4. CONCLUSION

Based on the analyses conducted in this study, it can be concluded that the dynamic motion behavior and mooring line responses of the system remain within the established design criteria, indicating that the overall stability and performance are satisfactory. From the standpoint of operational efficiency, the payout length of the mooring line can be further optimized by reducing the reserved laid length while maintaining appropriate safety factors. These findings suggest that the proposed decommissioning barge configuration demonstrates technical feasibility and suitability for implementation in Abandonment Site Restoration (ASR) operations.

ACKNOWLEDGMENTS

We extend our sincere gratitude for the support from the campus management of the Kalimantan Institute of Technology, especially the Institute for Research and Community Service (LPPM ITK). We also extend our gratitude to all relevant parties for their cooperation and support.

REFERENCES

[1] Tetteroo, D. (2022). Optimization of the lift point design decision-making process for offshore jacket decommissioning. Retrieved from https://repository.tudelft.nl/islandora/object/uuid%3A80e64288-b7404896-9fb34b36925dddc5

[2] Wiranto, J., & Migas, D. O. S. (n.d). Challenge & Opportunity of Platform Decommissioning in Indonesia Oil & Gas Upstream Business.

[3] itsjev. (2019, December 1). Alumni ITS Paparkan Urgensi Pembongkaran Anjungan Lepas Pantai. Retrieved 18 March 2024, from ITS News website: https://www.its.ac.id/news/2019/12/01/alumni-its-paparkan-urgensi-pembongkaran-anjungan-lepas-pantai/

[4] Fontaine, E., Kilner, A., Carra, C., Washington, D., Ma. K. T., Phadke, A., … Kusinski, G. (2014, May 5). Industry Survey of Past Failures. Pre-emptive Replacements and Reported Degradation for Mooring System of Floating Production Units. Presented at the Offshore Technology Conference. OnePetro. https://doi.org/10.4043/25273-MS

[5] American Petroleum Institute. (2005). Design and Analysis of Stationkeeping Systems for Floating Structures. USA: American Petroleum Institute

[6] DNV-GL. (2018). Marine operations and marine warranty. DNV-GL AS.

[7] Ellermann, K., & Kreuzer, E. (2003). Nonlinear Dynamics in the Motion of Floating Cranes. Multibody System Dynamics, 9(4), 377–387. https://doi.org/10.1023/A:1023361314261

[8] Kreuzer, E., & Mohr, A. (1997). Nonlinear dynamics of a moored crane barge in regular waves. Retrieved from https://www.osti.gov/etdeweb/biblio/634774

[9] Ren, H., Wang, X., Hu, Y., & Li, C. (2008). Dynamic response analysis of a moored crane ship with a flexible boom. Journal of Zhejiang University-SCIENCE A, 9(1), 26–31. https://doi.org/10.1631/jzus.A071308

[10] Schellin, T. E., Scharrer, M. E., & Matthies, H. G. (1982, May 3). Analysis of Vessels Moored in Shallow, Unprotected Waters. Presented at the Offshore Technology Conference. OnePetro. https://doi.org/10.4043/4243-MS

[11] Dianiswara, A. Analisis Respon Dinamis Gerakan dan Tali Tambat Crane Barge. Jurnaal Inovtek Polbeng, Vol.11, No. 1 Juni 2021. https://doi.org/10.35314/ip.v11i1.1897

[12] Aqwa Theory Manual. (2024).

[13] Design and Analysis of Stationkeeping Systems for Floating Structures: Upstream Segment : Addendum, May 2008. (2008). American Petroleum Institute.

[14] Gutiérrez Romero, J. E., García Espinosa, J., Serván Camas, B., & Zamora Parra, B. (2016). Non-linear dynamic analysis of the response of moored floating structures. Marine Structures, 49, 116–137. https://doi.org/10.1016/j.marstruc.2016.05.002

[15] Otori, H., Kikuchi, Y., Rivera-Arreba, I., & Viré, A. (2023). Numerical study of hydrodynamic forces and dynamic response for barge type floating platform by computational fluid dynamics and engineering model. Ocean Engineering, 284, Article 115100. https://doi.org/10.1016/j.oceaneng.2023.115100

copyright is published under Lisensi Creative Commons Atribusi 4.0 Internasional.